



## Use of a quartz microbalance for plasma–wall interaction studies

Daniel Bourgoin<sup>a,b,\*</sup>, Guy G. Ross<sup>a,b</sup>, Sylvio Savoie<sup>a,c</sup>, Yves Drolet<sup>a,d</sup>, Emile Haddad<sup>a,d</sup>

<sup>a</sup> Centre Canadien de Fusion Magnétique, Varennes, Qué., Canada J3X 1S1

<sup>b</sup> INRS-Énergie et Matériaux, Varennes, Qué., Canada J3X 1S2

<sup>c</sup> Canatom Inc., Montreal, Qué., Canada H3A 2A5

<sup>d</sup> MPB Technologies, Dorval, Qué., Canada H9P 1J1

### Abstract

This paper reports on the first use of quartz crystal microbalances as a useful diagnostic for plasma–wall interaction studies in tokamaks. Two quartz microbalance systems were installed recently in the TdeV tokamak. Reliable mass measurements are obtained when a correction is applied to the frequency response of the crystal, owing to its temperature rise during the discharges. Particle fluxes in the scrape-off layer (SOL), perpendicular and parallel to the magnetic field lines along the ion drift or electron drift directions were measured. As expected, a larger erosion rate was measured in the ion drift direction, while deposition was observed on the quartz surfaces facing up and facing down but not facing the plasma (i.e. field lines at grazing incidence). Radial displacement of the set-up permitted the measurement of the radial dependence of the erosion-deposition processes. An increase of the plasma current induces a slight increase of the deposit thickness. A detachment of the plasma in the divertor doubles the thickness of the deposit. The quartz microbalance showed that the deposition rate is strongly increased for a few discharges following a disruption. This diagnostic method is also sensitive to the atomic number of injected impurities.

*Keywords:* TdeV; Erosion and particle deposition diagnostic

### 1. Introduction

Important data for the understanding of dynamical phenomena such as erosion and redeposition on the walls can be obtained by the measurement of thickness variations of coating materials on a shot-to-shot basis in tokamaks. There are very few techniques to make such a measurement. Some authors propose the use of visible properties of matter to measure the coating thickness. One proposal is to use ellipsometry which measures the change in polarity of a reflected beam light to determine the film thickness [1]. Others use white light to illuminate the divertor region; they observe color changes as a function of film thickness

[2,3]. In the DIII-D tokamak some studies on a one shot basis have been done using the DIMES (divertor material evaluation system) facility [4,5] to expose different tiles in the divertor region to one discharge. Erosion and redeposition rates have been measured by using surface analysis of exposed tiles in the SOL (eg. Ref. [6]). Laser desorption has also been used in-situ in the TdeV tokamak [7]. A laser beam heats locally a tile between the shots and a calibrated mass spectrometer measures the quantity of the different hydrogen isotopes desorbed. Measurement of hydrogen retention in collector probes in the scrape-off layer has been done by this method. With these techniques, either the interpretation of the measurements is difficult, or the apparatus is expensive and complicated.

We propose a simple and powerful method that consists of exposing quartz crystal microbalances during tokamak discharges. Quartz microbalances have been used to measure different parameters in a variety of phenomena. For instance, this technique is widely used for the measurement of thin film thickness deposition under vacuum [8]

\* Corresponding author. Centre Canadien de Fusion Magnétique, Varennes, Québec, Canada J3X 1S1. Tel.: +1-514 929 8178; fax: +1-514 929 8102; e-mail: bourgoin@inrs-ener.quebec.ca.

and for the  $Q$ -factor measurement in gaseous and liquid environments [9]. The quartz microbalance is also used as a biosensor for detection of glucose using hexokinase [10]. Its principle is simple and well known [11]. It is a precise instrument that is able to measure thickness variation on a shot-to-shot basis in tokamaks. The microbalance can be used as is or better in combination with standard surface analysis techniques such as AES, XPS, RBS and ERDA.

This paper describes the use for the first time of quartz microbalances in a tokamak environment. Some typical results will be presented to illustrate the use of quartz microbalances as a useful diagnostic for plasma-wall interaction studies in tokamaks.

## 2. QCM characterization in laboratory

The erosion/deposition measurement by means of a quartz microbalance is based on its resonant frequency when an electric field is applied across a crystal. This frequency is lowered when a quantity of mass is deposited on it and increased when a quantity of mass is eroded from the quartz. The uncovered crystal has a resonant frequency around 6 MHz.

The resonant frequency of a crystal is also influenced by other parameters, the most important being the surrounding pressure and the temperature. Fig. 1 shows the temperature dependance of the resonant frequency of a crystal as measured by a thermocouple installed on the holder for different surrounding pressures. On the one hand, the pressure has negligible influence in our range of use ( $10^{-3}$ – $10^{-7}$  Torr). On the other hand, the temperature effect is under the company specifications and it is reproducible in the range from 50 to 95°C. All our measurements have been done in this range of pressure and temperature. Thus, there is no notable pressure dependence while a small correction has to be applied for temperature variation using the temperature dependance in Fig. 1. Note that the crystal temperature should not exceed its Curie temperature (573°C) as it loses its piezo-electric properties.

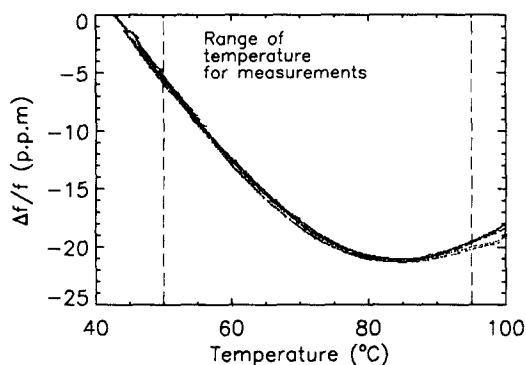


Fig. 1. Temperature dependance of a quartz crystal at varied pressures ( $10^{-3}$ ,  $10^{-4}$ ,  $10^{-5}$  and  $10^{-7}$  Torr).

## 3. Measurements in a tokamak

The TdeV tokamak is a medium size machine operated with divertors in a single null configuration. It has a major radius of 0.87 m and a minor radius of 0.27 m. Fig. 2 presents schematic views of TdeV and shows the position of the microbalances and rf-antenna. Tokamak discharges in TdeV last 1 s and deuterium ( $^2\text{H}_1$ ) gas is used both for the prefill and for maintaining the density constant. The walls are essentially made of stainless steel with graphite limiters and the rf-antenna is made of copper. A coating of boron is also deposited on the walls. Boronization [12,13] by glow discharge with 3–4% of  $\text{B}_2\text{D}_6$  (D stands for deuterium) in He was applied for our experiments at every 150 shots approximately. The temperature at the vessel varied from 30 to 50°C approximately.

An averaged 2000 Å thick film of amorphous carbon was deposited on each crystal before exposure to tokamak discharges. Each point plotted in the following graphs (Figs. 3–8) is the difference of the coating mass measured before and after one tokamak discharge except for Fig. 7 where a point stands for an average of five discharges (2 discharges for the chromium). The radial distance of the crystal from the separatrix is 5 cm unless otherwise specified. The setups were located on the mid-plane at two different toroidal positions (Fig. 2). When no rf-heating was used the antenna was pulled back behind the liner. The probe surface and the vessel walls are electrically grounded.

### 3.1. Measurements parallel to magnetic flux lines but not facing the plasma and perpendicular to the magnetic flux lines

The setup used for this section is named B on Fig. 2. Fig. 3 shows thickness variation as a function of the crystal orientation in the scrape-off layer of TdeV. When the crystal was facing up ( $90^\circ$ ) and down ( $270^\circ$ ), parallel to the  $B_t$  direction, a negative frequency shift was measured which means that particles are deposited on the crystal. For these experiments, the crystal was at a distance of 5 cm from the separatrix. Then, the crystal was positioned at a distance of 6 cm from the separatrix because the crystal broke at 5 cm. When the crystal was facing the ion-drift direction ( $0^\circ$ ), a positive frequency shift was observed which corresponds to a strong erosion of the film. When the crystal was facing the electron-drift direction ( $180^\circ$ ), only a small erosion was measured. Guo et al. [14] have shown that particle fluxes on the ion side of a probe exposed in TdeV are higher than those on the electron side. We estimate that the temperature on the crystal is kept under 200°C. So, the higher particle flux on the ion side is consistent with the stronger erosion measured by the microbalance.

## Cross sections

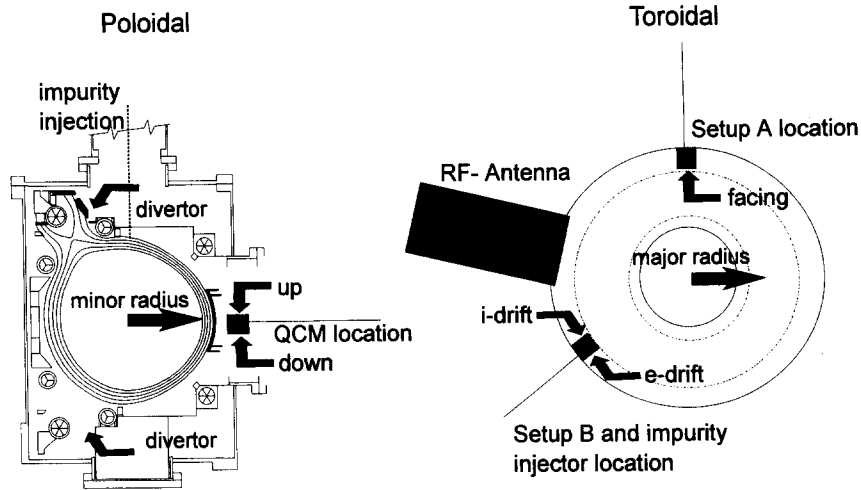


Fig. 2. Poloidal and toroidal cross sections of TdEV showing quartz crystal microbalance (QCM) and impurity injector locations.

### 3.2. Measurements parallel to the magnetic field lines and facing the plasma

The setup used for the next section is named A on Fig. 2. Results obtained for crystals exposed parallel to the magnetic field lines and facing the plasma are presented in this section. Fig. 4 shows the variation of thickness as a function of the distance of the crystal quartz from the separatrix. The distance was varied from 7 to 4 cm. In this range, deposition is the main process and the deposition rate increases when the distance is reduced. However, erosion has been observed in some particular conditions such as during rf-heating; these results are not shown in Fig. 4. When deposition is measured locally it does not necessarily mean a global behaviour for all the walls of the machine. On the contrary, the microbalance is probably located at a spot where redeposition of materials eroded from some other parts of the machine occurs. X-ray photo-

electron spectroscopy (XPS) analysis has been done on some typical quartz samples exposed to tokamak discharges. It showed the presence of boron, copper and carbon. The only possible source of boron in TdEV is the thin film deposited during boronization of the walls before tokamak discharges. The only source of copper is the rf-antenna which is located 90° further toroidally. Graphite limiters and divertor plates are an important source of carbon. All these statements support the conclusion that material is eroded from some parts in TdEV and redeposited on others such as the microbalance. We have no explanation for the two different points at 4 cm and no reason to reject either one of them. The 2 points were measured during 'identical' discharges and the upper one was measured first.

Fig. 5 shows the variation of thickness as a function of the plasma current ( $I_p$ ). The thickness of the deposited film was found to increase linearly with  $I_p$ . Measurement

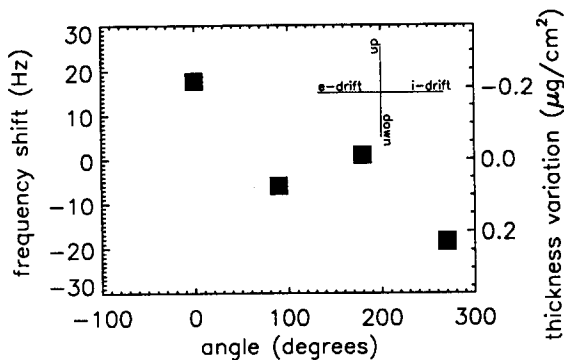


Fig. 3. Frequency shift and deposition thickness as a function of the orientation of the crystal ( $P_{HF} = 800$  kW,  $B_t = 1.8$  T,  $I_p = 180$  kA and  $n_c = 2-4 \times 10^{19} \text{ m}^{-3}$ ).

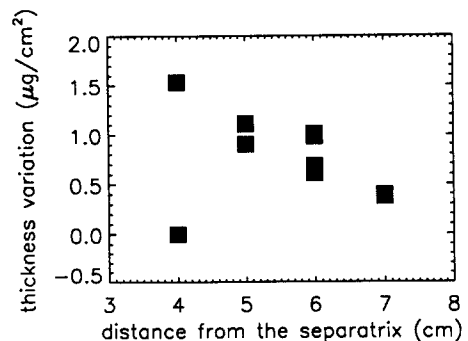


Fig. 4. Deposition thickness as a function of the radial distance from the separatrix ( $B_t = 1.4$  T,  $I_p = 180$  kA and  $n_c = 2 \times 10^{19} \text{ m}^{-3}$ ).

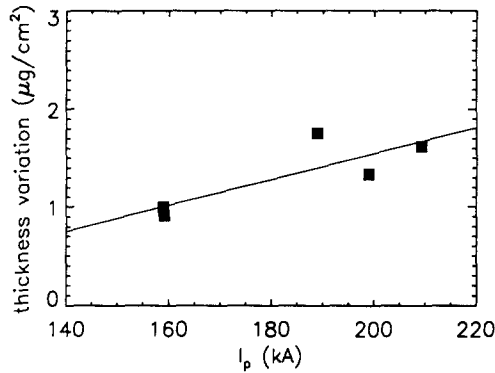


Fig. 5. Deposition thickness as a function of plasma current ( $B_t = 1.4$  T and  $n_e = 2 \times 10^{19} \text{ m}^{-3}$ ).

of the electron density at the separatrix with the lithium laser ablation diagnostic [15] shows a similar increase with  $I_p$  [16].

The variation of thickness as a function of the line-averaged electron density ( $n_e$ ) is shown in Fig. 6. When the plasma is attached to the divertor plate, the deposition rate does not vary with  $n_e$ . However, at higher density, a steep increase (the deposition doubled) was measured. At this density, the plasma is detached from the divertor plates while the electron density at this radius was 50% higher, as measured by the lithium laser ablation diagnostic method [17].

### 3.3. Impurity injection experiments

Impurities have been injected by means of laser ablation (ruby laser, 1.5 J, 30 ns) in the TdeV SOL. The diameter of the laser spot was 2 mm and Table 1 shows the thickness of the different impurity targets. Fig. 7 shows the measurement of the thickness variation of the film as a function of the atomic number of the injected impurity. Each point stands for an average of 5 measurements except for chromium for which only two measurements were

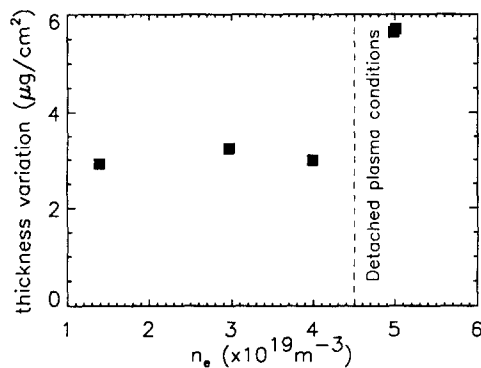


Fig. 6. Deposition thickness as a function of line averaged electron density ( $B_t = 1.8$  T,  $I_p = 180$  kA).

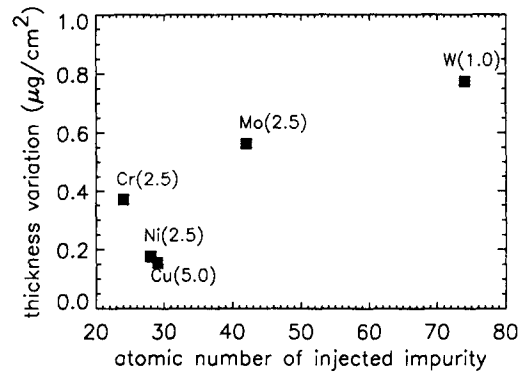


Fig. 7. Deposition thickness as a function of the atomic number of injected impurity ( $P_{\text{HF}} = 600$  kW,  $B_t = 1.8$  T,  $I_p = 190$  kA and  $n_e = 2\text{--}4 \times 10^{19} \text{ m}^{-3}$ ).

obtained. The quantity of matter deposited onto the crystal generally increases with the atomic number of the injected impurity. Two hypotheses can explain this result. First, the variation of thickness could be due to the deposition of the injected impurity and so, the greater the mass of the impurity, the more the thickness variation is high. Second, heavier impurities induce a stronger erosion by sputtering and thus a larger redeposition on the crystal. An analysis of the surface can distinguish between the two hypotheses. The quartz crystals were analyzed by Rutherford backscattering spectrometry and very few impurities were found on the crystal. We conclude that injection of heavier atoms such as tungsten induce much more erosion and redeposition than the injection of lighter atoms such as copper; this different behaviour was measured with the microbalance. We have no explanation for the increase of deposition when chromium atoms were injected. Table 1 also shows the approximate quantities as measured by RBS and analyzed with the GISA program [18].

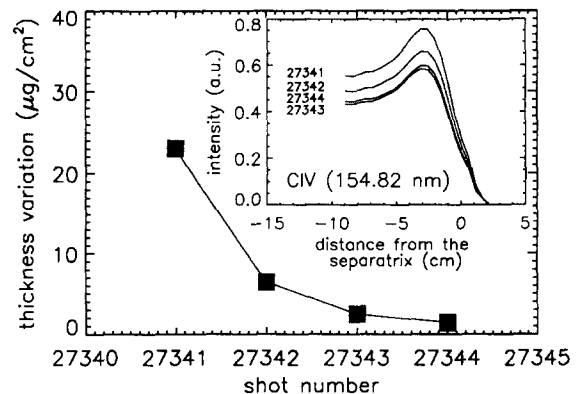


Fig. 8. Deposition thickness as a function of shot number for a reproducible series. Shot 27340 is a disruption. Insert: 1548.2. A carbon emission line intensity as a function of the distance to the separatrix. ( $B_t = 1.4$  T,  $I_p = 170$  kA and  $n_e = 4.5 \times 10^{19} \text{ m}^{-3}$ ).

Table 1

Impurity target thickness and approximate measured quantities found on the crystals for the impurity injection experiments as measured by RBS and analyzed with GISA

Elements	Target film thickness of injected impurity ( $\times 10^{-6}$ g/cm <sup>2</sup> )	Total quantity as measured by RBS ( $\times 10^{-6}$ g/cm <sup>2</sup> )
W	1900	0.04
Mo	2400	0.04
Cu	4500	0.45
Cr	1800	0.24
Ni	2200	0.12

### 3.4. Wall conditioning

It is now accepted that wall-conditioning is of prime importance for improved tokamak performances (see Ref. [19] for instance). During normal discharges, the wall is eroded at specific locations and the eroded material is redeposited at other locations. It is known that disruptions can reduce the benefits of wall-conditioning. Disruptions result in erosion and redeposition occurring at locations inside the vacuum vessel different from non-disrupted plasmas. Results of the microbalance show the importance of this phenomenon on wall conditioning. Fig. 8 shows the thickness variation measured for 4 reproducible shots following a disruption. A much higher deposition rate was measured immediately after the disruption. Stabilized conditions were obtained after approximately 4 shots. The 1548.2 Å carbon emission line was observed for these shots and the results plotted in the insert of Fig. 8. It is shown that a higher emission was measured which is in agreement with the measurements by the quartz microbalance. It is worth mentioning that no significant changes were observed in the other plasma parameters such as the loop voltage, in spite of the fact that those shots were very different in terms of wall-conditioning. It should be noted that the crystal sensitivity is nearly constant up to 2 mg/cm<sup>2</sup>. Thus, it does not play a role in these results.

## 4. Conclusion

A new diagnostic technique for the measurement of erosion and redeposition rates in tokamaks on a shot-to-shot basis has been developed in TdeV. Reliable measurements can be obtained when a small correction is applied for the variation of crystal temperature. When crystals are perpendicular to magnetic flux lines, strong erosion is measured in the ion-drift direction, weak erosion is observed in the electron direction, while deposition is measured on both the top and bottom sides. When the crystals face the plasma, the deposition increases quasi-linearly with the distance to the plasma. It was also recorded that the deposition rate increases linearly as a function of the plasma current and is constant as a function of the line-

averaged density except in the detached plasma regime, where a deposition rate twice as high is measured. Measurements obtained during injection of impurities show that the redeposition rate increases as a function of the atomic number of the injected impurity. This is explained by an increase of the erosion enhanced by heavy impurities at other spots inside the vacuum chamber. Finally, the effect of a disruption on wall-conditioning was recorded; this induces a much higher redeposition rate than during a well conditioned plasma discharge. These results confirm that the quartz microbalance is a promising tool in the study of plasma-wall interactions in tokamaks.

## Acknowledgements

D.B. wants to thank the Fonds FCAR for financial support. Authors wish to thank the TdeV team and especially J.-M. Guay and P. Trahan for technical support in data acquisition and analysis, G. Veilleux for helping with the XPS and J. Pelletier for the maintenance of the accelerator. The Centre Canadien de Fusion Magnétique is a joint venture of Hydro-Québec, AECL and INRS, in which MPB Technologies and Canatom also participate. It is principally funded by AECL, Hydro-Québec and INRS.

## References

- [1] S.J. Davies and R.D. Monk, *J. Nucl. Mater.* 196–198 (1992) 184.
- [2] P. Wienhold et al., *J. Nucl. Mater.* 220–222 (1995) 452.
- [3] G.L. Jackson et al., *Bull. Am. Phys. Soc.* 40 (1995) 1834.
- [4] C.P.C. Wong et al., *Bull. Am. Phys. Soc.* 40 (1995) 1792.
- [5] C.P.C. Wong et al., *J. Nucl. Mater.* 196–198 (1992) 871.
- [6] P. Wienhold et al., *J. Nucl. Mater.* 176–177 (1990) 150.
- [7] H.Y. Guo and B. Terreault, *Rev. Sci. Instrum.* 64 (1993) 701.
- [8] J. Janata, *Principles of Chemical Sensors* (Plenum Press, New York, 1990) p. 55.
- [9] M. Rodahl et al., *Rev. Sci. Instrum.* 66 (1995) 3924.
- [10] S.J. Lasky and D.A. Buttry, in: *Chemical Sensors and Micro-instrumentation*, ACS Symp., series 403 (American Physical Society, Washington, DC, 1989) p. 237.
- [11] C.-S. Lu and O. Lewis, *J. Appl. Phys.* 43 (1972) 4385.

- [12] J. Winter et al., *J. Nucl. Mater.* 162–164 (1989) 713.
- [13] C. Boucher et al., *J. Nucl. Mater.* 196–198 (1992) 587.
- [14] H.Y. Guo et al., Internal Report, CCFM RI 417e.
- [15] D. Michaud et al., *Rev. Sci. Instrum.* 63 (1992) 5698.
- [16] D. Bourgoin, Internal Report, CCFM RI 449f.
- [17] B. Terreault et al., these Proceedings, p. 755.
- [18] J. Saarihahti and E. Rauhala, *Nucl. Instrum. Methods B* 64 (1992) 734.
- [19] J. Winter et al., *Plasma Phys. Controlled Fusion* 36 (1994) b263.